JOURNAL OF THERMOPHYSICS AND HEAT TRANSFER
Vol. 10, No. 2, April–June 1996

Convective Instabilities in Rarefied Gases by Direct Simulation Monte Carlo Method

E. Golshtein* and T. Elperin†
Ben-Gurion University of the Negev, Beer Sheva 84105, Israel

Benard and thermal stress instabilities in a rarefied gas are investigated by the direct simulation Monte Carlo (DSMC) method. Particular emphasis is given to the numerical aspects of DSMC (accuracy, convergence, etc.), that were not investigated in the previous studies and to the refining of the simulation results by using a special data processing (filtering) procedure. In the stratified rarefied gases with high-temperature gradients the Boussinesq approximation is not valid and it is shown that the onset of instabilities in the non-Boussinesq fluid (rarefied gas) is not determined by a single nondimensional parameter (Rayleigh number). Benard convection in the stratified rarefied gas is analyzed in different geometries, including the case with curvilinear boundaries. The occurrence of thermal stress convection in rarefied gases and in a continuum flow regime under zero gravity conditions was demonstrated using the DSMC method.

Nomenclature

a = speed of sound
d = distance between plates
$\langle E \rangle$ = volume-averaged normalized energy of molecule
Fr = Froude number
f = particles distribution function in phase space
g = acceleration of the external force
Kn = Knudsen number
m = molecular mass
N = number of molecules in simulation
R = gas constant
Ra = Rayleigh number
$\overline{Ra}$ = average Rayleigh number
r_T = temperature ratio, T_c/T_h
r_ρ = density ratio, $\rho_{\min}/\rho_{\max}$
s = nondimensional form parameter
T_c = cold plate temperature
T_h = hot plate temperature
T_ω = temperature of the body
$\langle u \rangle$, $\langle v \rangle$ = volume-averaged normalized velocity components in the x and y direction
u, v, w = velocity components in x, y, and z direction
v_{th} = most probable thermal speed
β = temperature gradient in the vertical direction
Γ = aspect ratio
γ = specific heats ratio
λ = mean free path
λ_{cr} = critical wave number
ρ = density
ρ_h = hot plate density
τ = mean free flight time, λ/v_{th}
ω = variable hard sphere exponent

Introduction

THE onset of Benard instability in the Boussinesq approximation was studied analytically and numerically in many works.[1] The main purpose of this study is to investigate this instability in the rarefied gases by the direct simulation Monte Carlo (DSMC) method. Boussinesq approximation is valid only in the limit of infinitely small temperature differences,[2] whereas in rarefied gases instabilities are excited when the temperature differences are large and variations of physical properties with temperature must be taken into account.

Benard instability in rarefied gases has been investigated previously by the molecular dynamics (MD) method[3–5] and by the DSMC method.[6,7] It has been shown that the DSMC method allows one to resolve vortex patterns in a flowfield. The DSMC method is the most widely used numerical technique for analyses of flows of rarefied gases.[8] However, the application of the DSMC method to calculate the flow pattern in Benard convection requires very high accuracy. Indeed, our analysis of some of the reported in literature results on the DSMC calculation of Benard convection flows showed that the velocity of the convective rolls was comparable or even less than a statistical error. The main goal of this study is to analyze the accuracy and convergence of the DSMC method in calculating convective flows in rarefied gases.

Benard Instability

Benard instability arises because of the instability of the purely conducting state of a fluid heated from below in a gap between two parallel horizontal plates under the action of a constant external force. Linear perturbation analysis of the governing equations in the Boussinesq approximation shows that a single dimensionless parameter (Rayleigh number) determines the stability of the system.[9] In most of the investigations of Benard's instability, the Boussinesq approximation was valid. In this study we investigate the Benard's instability in a rarefied gas. Notably, in the rarefied gas the Boussinesq's approximation is not valid any more while the solution of the Navier–Stokes equations becomes very difficult. The main goal of this study is to investigate convective instabilities in rarefied gases numerically using the DSMC method.

We start our analysis of the numerical results from a one-dimensional conductive state. Each collision cell initially contained 15–50 simulated particles. The computational domain was divided into 100 collision cells. The cell's size is equal to the mean free path. Initial molecule's velocities are sampled from the equilibrium Maxwellian distribution, and each cell contains the same number of particles. Diffuse and specular reflection boundary conditions are assumed at upper/lower wall and side boundaries, respectively. After each time step

Received April 13, 1995; presented as Paper 95-2054 at the AIAA 30th Thermophysics Conference, San Diego, CA, June 19–22, 1995; revision received Dec. 7, 1995; accepted for publication Dec. 7, 1995.

*Ph.D. Student, Pearlstone Center for Aeronautical Engineering, P.O. Box 653.
†Associate Professor of Mechanical Engineering, Pearlstone Center for Aeronautical Engineering, P.O. Box 653. Member AIAA.

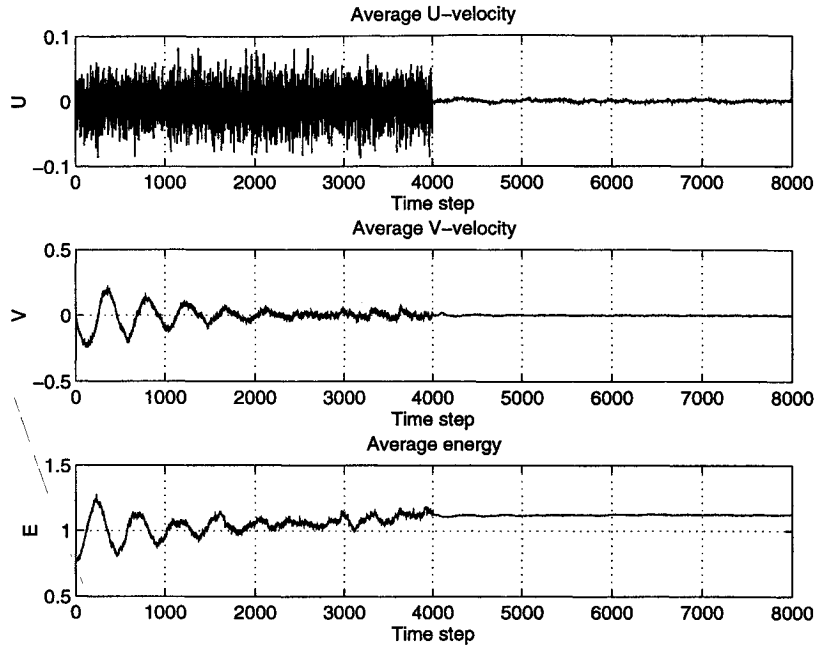

Fig. 1 Average characteristics of the flow with stratification vs time in the case when a two-dimensional simulation is started from a one-dimensional approximation.

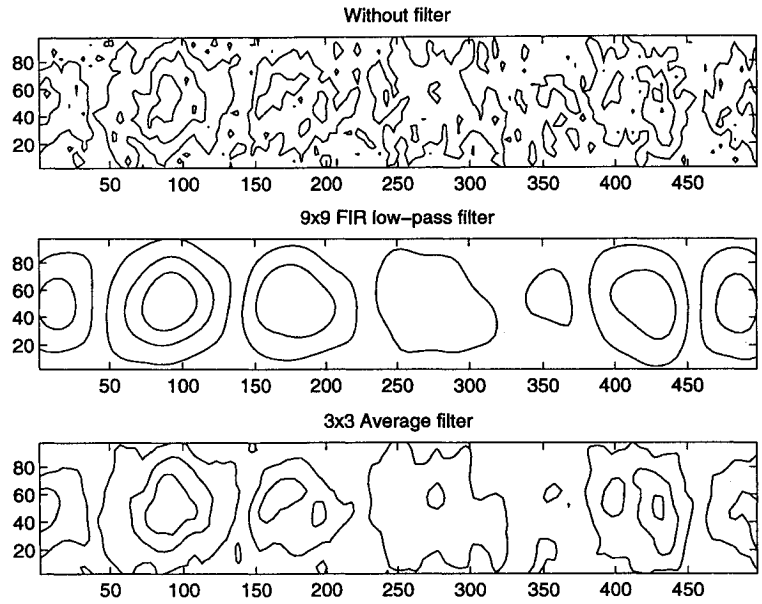

Fig. 2 Contour lines of the velocity component $V(x, y)$ obtained with different filtering procedures.

the volume-averaged normalized (by v_{th}) velocity components in the x and y directions $\langle u \rangle$, $\langle v \rangle$, and $\langle E \rangle$, which determine the average temperature of a flow, are calculated. The flow is considered steady (time independent) if these average characteristics of the flow exhibit only statistical fluctuations. Temperature distribution with high temperature ratio $r_T = T_c/T_h = 0.2$, obtained after 10,000 time steps (each time step is 0.7 of the mean free flight time $\tau = \lambda/v_{th}$, where the most probable v_{th} is calculated at the hot plate temperature), is in a good agreement with the analytical solution

$$T = T_0 - \beta y \tag{1}$$

In the case with strong stratification $r_\rho = \rho_{min}/\rho_{max} \approx 0.02$, the calculated equilibrium density distribution is in good agreement with analytical solution:

$$\rho/\rho_0 = [1 - (1 - r_T)(y/d)]^{[2/(1-r_T)Fr]-1} \tag{2}$$

where $Fr = (2RT_h/gd)$ is the Froude number calculated at the hot plate temperature.

In the case with high stratification, two-dimensional simulation is started from the equilibrium Maxwellian distribution and with constant density (equal number of simulated particles in each cell). Because of high acceleration caused by the external force, high-amplitude oscillations appear in the flow. These oscillations are clearly observed in the plot of the volume-averaged velocity components and energy vs number of time steps (see Fig. 1). As can be seen from this plot the oscillations are damped after sufficiently long time (2000 time steps). Clearly, the employed initial state of a gas is not realistic for the analysis of the onset of the Benard instability in the case with stratification, and it is difficult to separate the oscillatory motion from the convective flow. To eliminate these undesirable oscillations we used a more realistic initial state, whereby we started two-dimensional calculations from the

one-dimensional approximation and the oscillations were completely eliminated (see Fig. 1).

Flow properties $\rho(x, y)$, $T(x, y)$, $V(x, y)$ (density, temperature, and velocity components), determined in the course of simulation, are subjected to statistical fluctuations. To decrease these fluctuations we used a time-averaging procedure. In the calculations two samplings are used: a short-time sampling (every 600 time steps) and a long-time sampling, which in some cases reached 50,000 time steps. In addition, for smoothing the results, the sampled flow properties were averaged over 5×5 collision cells.

When the flow is steady, the long-time averaging produced very good results with small statistical fluctuations. However, if the flow is time dependent,[4,5] long-time averaging cannot reproduce the real flow since the averaging procedure yields some averaged flow. The flow velocity in the Benard instability problem is relatively slow (about 0.1 of the v_{th}), and when statistical fluctuations are large, the resulting flowfield cannot be resolved. Therefore, the sample size must be very large and to observe formation of the convective rolls pattern, a long simulation time (2000–4000 of the mean free flight time) is needed. However, the number of particles in simulation is limited since the simulation time necessary for convective cells formation grows with the number of particles. On the other hand, since the flow is unsteady, the time-averaging interval must be as short as possible.

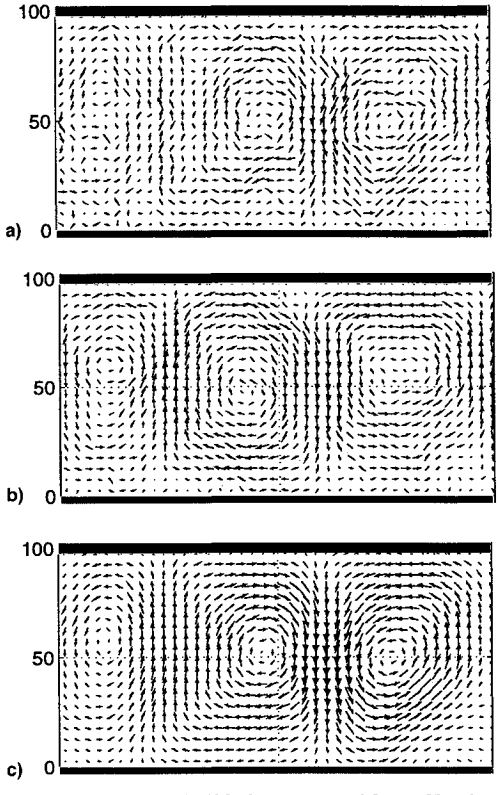

Fig. 3 Averaging over a) 600 time steps without filtering, b) 9600 time steps without filtering, and c) 600 time steps with filtering.

To reduce the calculation time and improve the quality of the simulation results by separating (filtering) the low-frequency flow velocity from the high-frequency statistical fluctuations, a method of digital image filtering[10] was used. The input data for filtering is a two-dimensional function of the flow properties in each cell. Image filtering can be performed in the Fourier frequency space. In this case the image is transformed to the Fourier space and is filtered in this space. The low-frequency flowfield spectrum is separated using a low-pass filter. A more simple method is filtering directly in the real space. In the latter case a mask matrix is moved pixel-by-pixel over the image. In Fig. 2 we compared results obtained with a 3×3 pixel mask average filter and two-dimensional 9×9 low-pass finite impulse response (FIR) filter. The filtered flow property $\tilde{P}_{kj}$ in a cell k, j is obtained as follows:

$$\tilde{P}_{kj} = \frac{1}{M^2} \sum_{m=1}^{M} \sum_{n=1}^{M} \{K_{mn} P_{k-[(M-1)/2]+m, j-[(M-1)/2]+n}\} \qquad (3)$$

where P_{ij} is a flow property in a cell i, j before filtering; K is the mask matrix; and M is the number of rows in the mask matrix. In the case of the average filter, matrix K is the matrix of ones.

In Fig. 2 we show results obtained after application of filtering the velocity component $V(x, y)$. However, the flow pattern is better visualized by streamlines. For filtering the streamline image we used the previously filtered velocity fields $U(x, y)$ and $V(x, y)$ as input for plotting the streamlines. In Fig. 3 the results obtained after short-time averaging (600 time steps) with filtering are compared with those obtained by long-time averaging without filtering (9600 time steps).

Formation of a convective flow pattern in a domain with $\Gamma = 5$ is shown in Fig. 4. The domain is divided into the 100×500 collision cells and 20×100 sampling cells. Each collision cell contains five simulated particles. Calculation is started from one-dimensional approximation. In simulation we used the variable hard sphere (VHS) model[8] with $\omega = 0.66$ for a gas with $m = 6.65 \times 10^{-26}$ kg, $\gamma = 1.667$, and viscosity 1.865×10^{-4} at temperature 273 K. The cold plate temperature is $T_c = 40$ K, the distance between plates is $d = 0.05$ m, the Knudsen number is $Kn = 0.01$, the Froude number is $Fr = 4$, and the temperature ratio is $r_T = 0.5$. Sampling is started after 2400 time steps. The flow properties are averaged over 10,000 time steps. The wave number of the Benard's rolls that is shown in Fig. 5 is about 2. This value is in a good agreement with the critical wave number obtained by linear analysis using Boussinesq approximation $\lambda_{cr} = 2.03$. However, in many numerical experiments with $\Gamma = 2$ we observed steady three roll patterns (see Fig. 5). Therefore, in some cases the wave number $\lambda_{cr} < 2.03$, and it is in compliance with other DSMC simulations.[6] In several cases we observed only one roll (see Fig. 5). The observed numerical simulation values of the wave numbers less than the critical value can be caused either by the error induced by the periodic boundary conditions for $\Gamma = 2$ in the simulations or by rarefied gas effects.

To eliminate density gradient in the pure conduction state

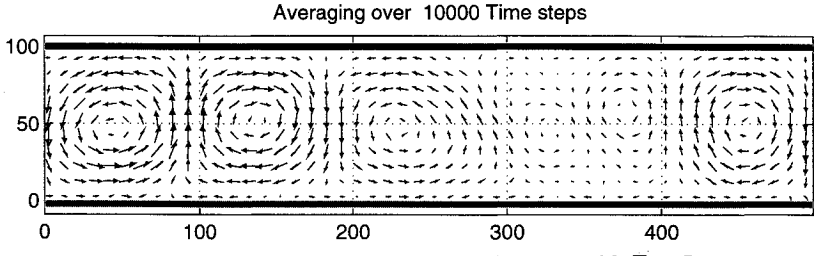

Fig. 4 Formation of cellular patterns in a gap with $\Gamma = 5$.

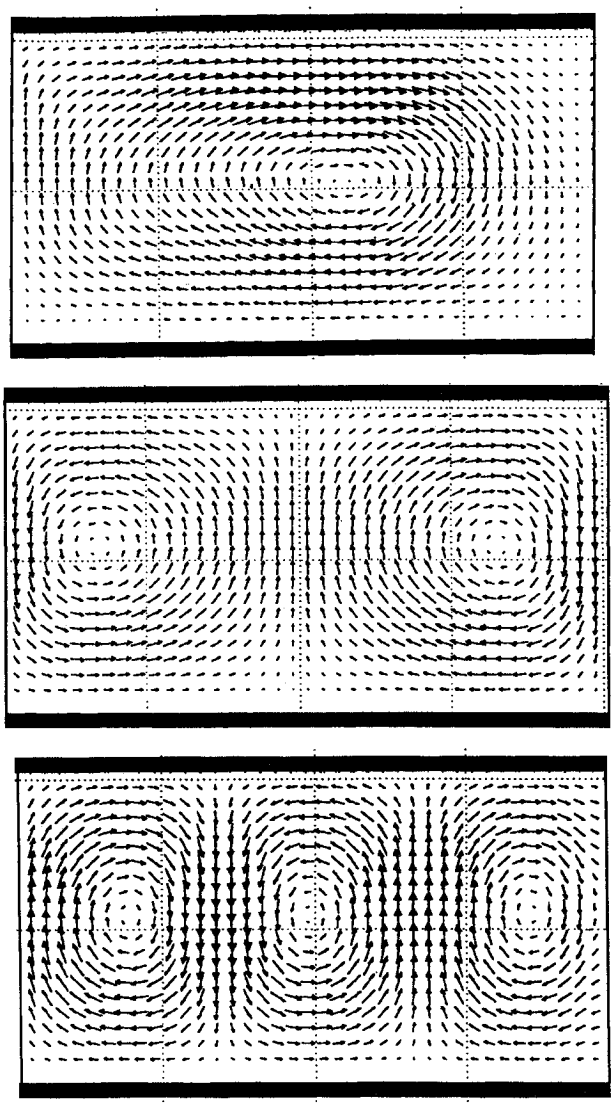

Fig. 5 Different roll patterns in a gap with $\Gamma = 2$.

we used Eq. (2) for the density distribution. This equation implies that if

$$(g/\beta R) - 1 = 0 \tag{4}$$

then the density is constant.[11] The flow pattern is determined by temperature ratio, $Kn = (\lambda/d)$, d, and T_c. The appropriate acceleration of the external force field is calculated from Eq. (4). Calculated density distribution in a case when condition (4) is satisfied is shown in Fig. 6. As can be seen from this plot, the density is nearly constant, with slight deviations except for the cold plate boundary. However, the temperature ratio at critical Rayleigh number is quite high ($r_T = 0.5 \div 0.7$), and properties of fluid vary significantly in the vertical direction. To account for this variation we defined the effective or average Rayleigh number using the assumption that the temperature profile is linear in the vertical direction (see Fig. 6) and $T_{av} = (T_h + T_c)/2$. The kinematic viscosity and heat diffusivity are calculated from the Chapman–Enshog theory for hard spheres. Then the formula for Rayleigh number reads,

$$Ra = \frac{512}{75\pi}\frac{\Delta T}{T}\frac{d^3 g}{\lambda^2 2RT} \tag{5}$$

The formula for the average Rayleigh number calculated at T_{av} temperature (taking into account that λ = const when the number density is constant for a hard sphere model), reads,

$$\overline{Ra} = \frac{2048}{75\pi}\frac{(1 - r_T)}{(1 + r_T)^2}\frac{d^3 g}{\lambda_0^2 2RT} = \frac{8.692(1 - r_T)}{FrKn^2(1 + r_T)^2} \tag{6}$$

where the Froude number is calculated at the hot plate temperature.

It can be expected that in the vicinity of critical Rayleigh numbers the convection flow is very slow. Numerical results show that roll formation at the values of Rayleigh number in the vicinity to the critical value strongly depends upon the statistical fluctuations in the simulation. Convective flow pattern at Rayleigh number 1150 with long-time averaging (36,000 time steps) is resolved. However, at short-time averaging (each 600 time steps) the pure conduction state is ob-

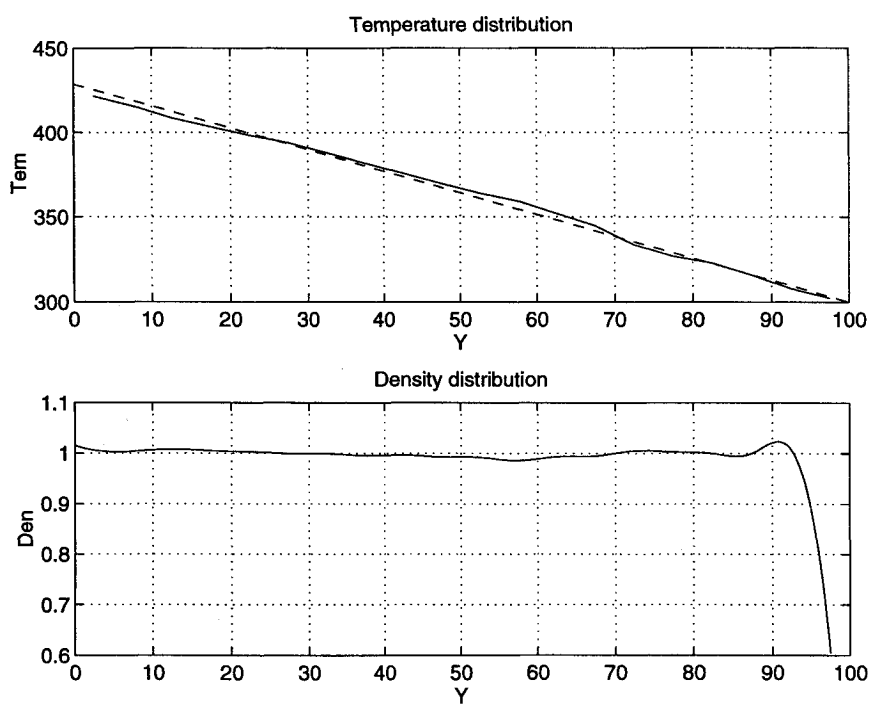

Fig. 6 Temperature and density distribution at $r_T = 0.7$ and $Kn = 0.01$ [Eq. (4) is satisfied].

served. Therefore, the flow instability is resolved and observed in calculations only within the limits of the statistical error. The latter determines the minimum flow velocity that can be resolved in the calculation. In this study only rolls with an average velocity at least 3 ÷ 5 times greater than volume-averaged standard deviation of the velocity components were observed.

In the calculations two parallel sampling procedures were employed: over a short-time interval (600 time steps) and averaging over a long time (in some calculations 50,000 time steps). In several cases after filtering, the observed gas flow was caused by statistical fluctuations. If the average flow velocity obtained in the calculations scales as $v_{av} \propto (\sqrt{N})^{-1}$, it can be safely concluded that the system is in a pure conduction state and the observed flow is the result of the statistical fluctuations.

Watanabe et al.[12] studied Benard's instability in the rarefied gas by the DSMC method. The bifurcation region between convective and conductive state was calculated by comparison temperatures at different locations in the computational domain, and it appeared to agree with the critical Rayleigh number for a rigid boundary condition obtained by linear analysis, i.e., $Ra = 1700$. The critical Rayleigh number that is determined in the present study is about 1100. This difference in critical Rayleigh number value may be explained by the significantly different conditions in a rarefied gas, which do not comply with the Boussinesq approximation and restrictions of the linear theory analysis. Benard instability in rarefied gases is always accompanied by strong stratification. It can be expected therefore that the density gradient has a significant effect on the bifurcation point between the conductive and convective states.

The direction and magnitude of the density gradient in the pure conduction state can be calculated from Eq. (2). The results of the simulations showed that if the density gradient is in the direction of the external force and the Rayleigh number is estimated from Eq. (6), then the critical Rayleigh number is significantly higher than 1700.

At Rayleigh number 4300 with long-time averaging (16,800 time steps), pure conduction state is observed. The parameters in the calculation are as follows: the HS molecule model is used, $Kn = 0.01$, $Fr = 2.1$, the temperature ratio is $r = 0.7$, the cold plate temperature is 4 K, five simulated particles are sampled in each collision cell at initial time, the distance between plates is 5 cm, and the computational domain is divided into 100×200 collision cells and 20×40 sampling cells. However, at higher Rayleigh numbers, convection rolls were detected. Thus, $Ra = 4300$ corresponds not to the turbulent regime, but to a pure conduction state. On the contrary, when the density gradient is in the direction opposite the external force, roll patterns are observed at $Fr = 10$, $r = 0.68$, and $Kn = 0.01$, which correspond to $Ra = 985$. These results demonstrate that the Rayleigh number is not a single dimensionless parameter that determines the bifurcation point between a conductive and a convective state, and estimations based on the average Rayleigh number are not valid in this case. One must take into account the density gradient in the vertical direction, because $\lambda \propto \rho^{-1}$ for hard sphere (HS) molecular model.

The onset of convective motion can occur also when the upper and lower boundaries are curvilinear. We used the

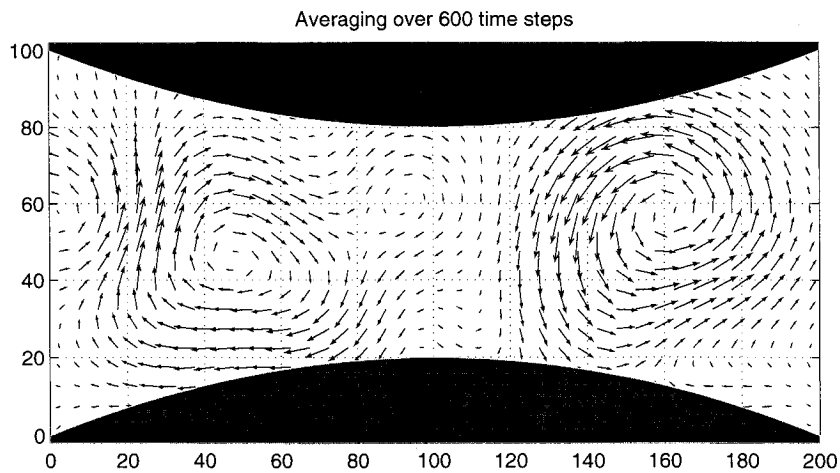

Fig. 7 Cellular patterns in a gap with curvilinear parabolic boundaries ($s = 0.2$) at $\overline{Ra} = 4829$.

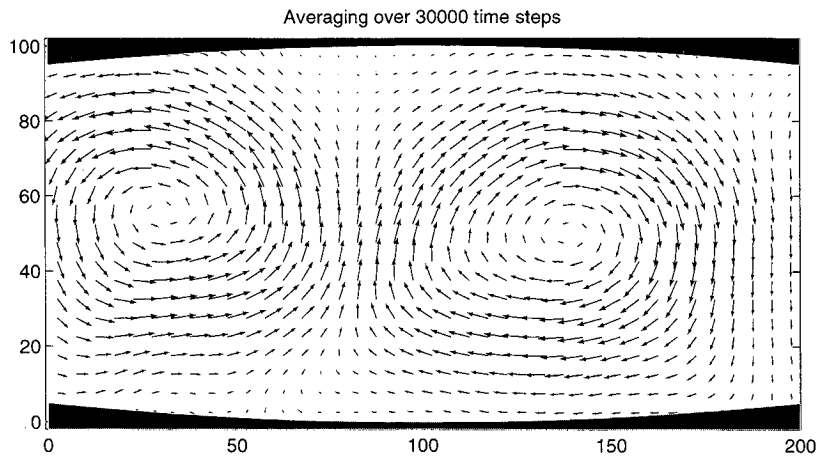

Fig. 8 Cellular patterns in the flow with curvilinear parabolic boundaries ($s = -0.05$) at $\overline{Ra} = 887$.

DSMC method to calculate Benard convection in a rarefied gas in this geometry. In simulation we used parabolic boundaries (see Fig. 7) with form parameter $s = l_m/d$, where l_m is the maximum (positive sign) or minimum (negative sign) location of a lower boundary. The average Rayleigh number is estimated at the point of maximum distance between boundaries. Flow pattern at $Ra = 4829$, $Kn = 0.01$, $r_T = 0.5$, $T_c = 200$ K, $Fr = 4$, and $s = 0.2$ is shown in Fig. 7.

Flow patterns at $Ra = 887$, $Kn = 0.01$, $r_T = 0.75$, $T_c = 200$ K, $Fr = 8$, and $s = -0.05$ are shown in Fig. 8. Calculations show that the onset of instability and flow patterns significantly depend upon the form of the boundaries (compare Figs. 7 and 8). The critical Rayleigh number calculated in the case of $s = -0.1$ is about 540. Simulation results clearly show that curvilinear boundaries promote the onset of instability and that fluid always rises at the location of a maximum distance between boundaries. The convective motion, as can be expected, disappears with increasing the Knudsen number. Calculations show that at $Kn = 0.05$, only pure conduction states are observed.

Thermal Stress Instability

The solution of the Boltzmann equation can be expanded into the power series of Knudsen number:

$$f(t, \bar{x}, \bar{\varepsilon}) = f^{(0)} + Knf^{(1)} + Kn^2 f^{(2)} + \cdots \tag{7}$$

The first-order approximation $[Knf^{(1)}]$ yields the Navier–Stokes solution. The second-order terms add correction terms (Burnett terms) to the Navier–Stokes equation. These terms can be neglected in most cases. However, there exists a class of flows where the thermal Burnett stresses[13] are of the same order of magnitude as the Navier–Stokes terms, and should be accounted for.

An important consequence of the temperature stresses is a thermal stress convection that occurs in the absence of external forces. If a uniformly heated body with temperature T_h is submerged into a gas with temperature $T_\infty \neq T_h$, then in the Navier–Stokes hydrodynamics without external forces the gas is at rest. However, when Burnett corrections are taken into account, convection flow appears because of thermal stresses. Thermal stress convection is the only kind of convection occurring in a gas phase under zero gravity conditions. Remarkably, thermal stress convection can be excited at $Kn \ll 1$, but it cannot be described using the Navier–Stokes equations. At $Kn \to \infty$, the thermal stress convection disappears. The convection flow velocity in thermal stress convection is rather small. However, actual velocities of the flow during thermal stress convection may be quite high, provided that the temperature is sufficiently high. The convection velocity is of the order of the characteristic viscous flow velocity based on the gasdynamic parameters near the body:

$$u \approx \mu/gL \approx Kn \cdot a \tag{8}$$

where a is the speed of sound at the hot wall temperature. For example, if the temperature of the body is $T_w = 3 \times 10^4$ K and $Kn = 0.1$, the flow velocity is of the order of 10^2 m/s.

The example of internal thermal stress convection is the flow between two wavy surfaces maintained at different temperatures. If the temperature difference is large enough, then convection may change the heat flux between the surfaces. We used the DSMC method for the analysis of thermal stress instability that arises in a gas between two curvilinear parallel infinite walls with different temperatures $T_c \ll T_h$, because of the temperature stresses under zero gravity condition. Certainly, in the limiting case $Kn \to \infty$, there is no convection. In simulation we used diffuse reflecting parabolic and sinusoidal hot and cold plates and periodic boundary conditions at the side boundaries. Values of the volume-averaged velocities of a convective flow obtained in simulations are in a compliance

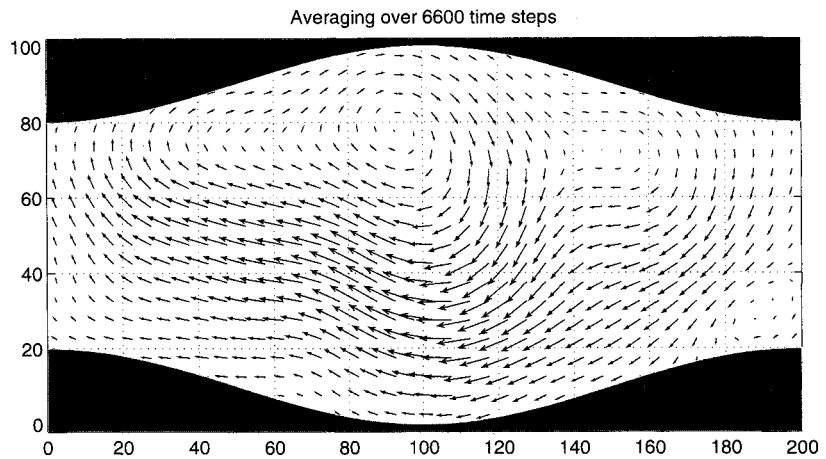

Fig. 9 Roll patterns in the thermal stress convection in a gap with $\Gamma = 2$ and sinusoidal boundaries $s = -0.2$. The cold plate temperature 300 K (upper boundary), the hot plate temperature 3×10^4 K (lower boundary), $Kn = 0.01$, and the average flow velocity is of order $0.0025v_{th}$.

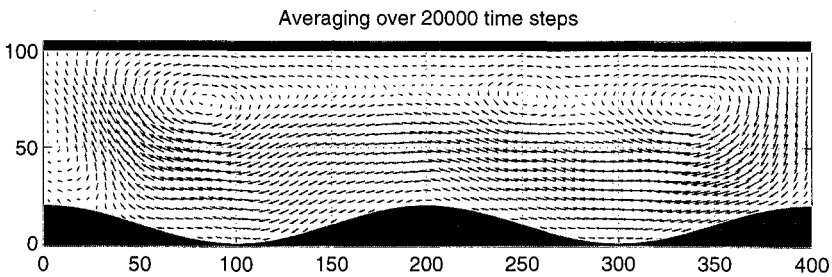

Fig. 10 Roll patterns in the thermal stress convection in a gap with $\Gamma = 4$. The cold plate temperature 300 K (upper boundary $s = 0$), the hot wall temperature 3×10^4 K (lower sinusoidal boundary $s = 0.2$), $Kn = 0.01$, and the average flow velocity is of order $0.002v_{th}$.

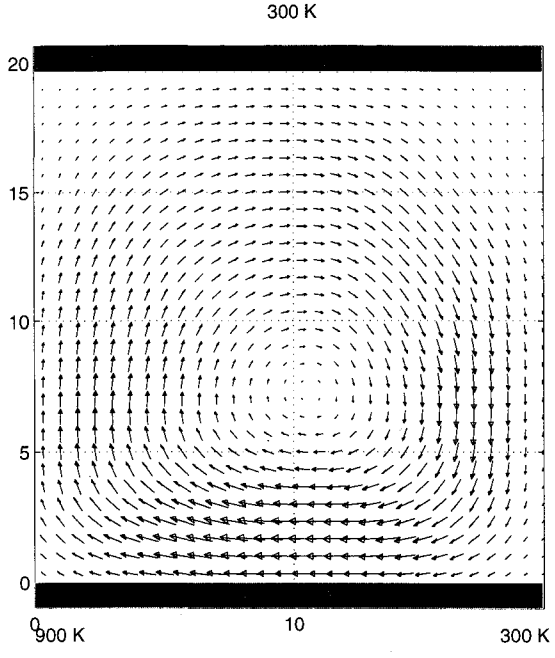

Fig. 11 Roll patterns in the thermal stress convection in a gap with $\Gamma = 1$. The cold plate temperature 300 K (upper boundary), the hot plate has temperature gradient 6000 K/m (lower boundary), $Kn = 0.05$, and the average flow velocity is of order $0.0035v_{th}$.

Eq. (8). Flowfields observed in simulations with different geometries are presented in Figs. 9 and 10.

Another example of the internal thermal stress convection is the flow between two flat plates, where one plate has a longitudinal temperature gradient and the other is kept at a constant temperature[14] (presented in Fig. 11). Calculations show that in this case of thermal stress convection the flow velocities are significantly higher than those observed in the thermal stress convection between two wavy surfaces.

Conclusions

In this study we investigated numerically Benard and thermal stress instabilities in rarefied gases. It was demonstrated that the DSMC method allows one to resolve the relatively slow vortex motion. The developed filtering procedure permits visualization of a slow convective flow with a high statistical noise. It was shown that in Benard convection the Rayleigh number that determined the onset of instability in Boussinesq fluid is not the only relevant parameter in stratified rarefied gas flow. The occurrence of the thermal stress convection in rarefied gases and in continuum flow regime under zero gravity conditions was demonstrated by the DSMC method.

References

[1]Koschmieder, E. L., *Benard Cells and Taylor Vortices*, Cambridge Univ. Press, Cambridge, England, UK, 1993.

[2]Gitterman, M., "Hydrodynamics of Fluids near a Critical Point," *Reviews of Modern Physics*, Vol. 50, No. 1, 1978, pp. 85–106.

[3]Puhl, A., Mansour, M. M., and Mareschal, M., "Quantitative Comparison of Molecular Dynamics with Hydrodynamics in Rayleigh-Benard Convection," *Physical Review A: General Physics*, Vol. 40, No. 4, 1989, pp. 1999–2012.

[4]Rapaport, D. C., "Time-Dependent Patterns in Atomistically Simulated Convection," *Physical Review A: General Physics*, Vol. 43, No. 12, 1991, pp. 7046–7048.

[5]Rapaport, D. C., "Temporal Periodicity in Microscopic Simulation of Rayleigh-Benard Convection," *Microscopic Simulations of Complex Hydrodynamic Phenomena*, edited by M. Mareschal and B. L. Holian, Plenum, New York, 1992.

[6]Stefanov, S., and Cercignani, C., "Monte Carlo Direct Simulation of Benard's Instability in a Rarefied Gas," *European Journal of Mechanics, B/Fluids*, Vol. 11, No. 5, 1992, pp. 543–553.

[7]Stefanov, S., and Cercignani, C., "Monte Carlo Simulation of the Taylor-Couette Flow of a Rarefied Gas," *Journal of Fluid Mechanics*, Vol. 256, 1993, pp. 199–213.

[8]Bird, G. A., *Molecular Gas Dynamics and Direct Simulation of Gas Flow*, Clarendon, Oxford, England, UK, 1994.

[9]Drazin, P. G., and Reid, W. H., *Hydrodynamic Stability*, Cambridge Univ. Press, Cambridge, England, UK, 1981.

[10]Kirsch, S., Griesche, J., and Gericke, W., "Monte-Carlo Simulation of the Beam Flux Distribution of Molecular-Beam Epitaxy Sources by Consideration of Intermolecular Collisions," *Physica Status Solidi: A*, Vol. 123, 1991, pp. 441–450.

[11]Garcia, A., and Penland, J., "Fluctuating Hydrodynamics and Principal Oscillation Pattern Analysis," *Journal of Statistical Physics*, Vol. 64, No. 5/6, 1991, pp. 1121–1132.

[12]Watanabe, T., Kaburaki, H., and Yokokawa, M., "Simulation of a Two-Dimensional Rayleigh-Benard System Using the Direct Simulation Monte Carlo Method," *Physical Review*, Vol. 49, No. 5, 1994, pp. 4060–4064.

[13]Kogan, M. N., "Kinetic Theory in Aerothermodynamics," *Progress in Aerospace Sciences*, Vol. 29, 1992, pp. 271–354.

[14]Ota, M., Tanaka, G., and Gao, P., "Rarefied Gas Flows Induced by Temperature Gradients on Solid Surface," *Proceedings of the 3rd Asian Symposium on Visualization*, edited by Y. Nakayama and T. Tanahashi, Visualization Society of Japan, Chiba, Japan, 1994, pp. 507–512.